Revista Brasileira de Geofísica
RBGf
Brazilian Journal of Geophysics

Revista Brasileira de Geofísica (2016) 34(3): 393-404
© 2016 Sociedade Brasileira de Geofísica
ISSN 0102-261X
www.scielo.br/rbg

REVISITING SOME OLD UNEXPLAINED EFFECTS IN INDUCTION LOGS WITHIN LAMINATED FORMATIONS WITH THE TRIAXIAL INDUCTION TOOLS

Paulo Roberto de Carvalho[1] and Cícero Roberto Teixeira Régis[2]

ABSTRACT. Modern induction triaxial or multicomponent well logging tools provide resistivity anisotropy logs, and estimates of the electrical resistivity of sand laminae in thinly laminated formations. In this paper, coaxial and coplanar vertical logs were modeled in one-dimensional (1D) laminated packages and in their equivalent anisotropic beds, neglecting the presence of the borehole and the invasion zones, to simulate geological environments of hydrocarbon reservoirs with resistivity anisotropy. The objective of this paper is twofold: to perform a quantitative analysis of the anisotropy level of a thinly laminated reservoir as compared to an equivalent anisotropic bed, and, in doing so, to revisit some old and unexplained effects that appear on the triaxial induction logs. These subtle effects may have only a faint influence on the logs themselves, but their study contribute to our understanding of the electromagnetic phenomena involved in the induction logging. The results show that the coaxial logs in the laminated formation converge to the equivalent anisotropic bed response much sooner than the coplanar logs. They also show that there is a considerable difference between the anisotropy index obtained by the triaxial induction tool within laminated formations and the anisotropy coefficient of its equivalent anisotropic bed, even for extremely thin laminae thicknesses.

Keywords: well logging, multicomponent induction tools, laminated reservoirs, electrical anisotropy.

RESUMO. As atuais ferramentas de perfilagem em poço por indução eletromagnética, denominadas triaxias ou multicomponentes, fornecem perfis de anisotropia elétrica e permitem estimar a resistividade de lâminas de areia em ambientes finamente laminados. Neste artigo, os perfis dos arranjos coaxial e coplanar de bobinas foram simulados em modelos unidimensionais (1D) de sequências laminadas e de suas respectivas camadas anisotrópicas equivalentes, negligenciando o poço e as zonas de invasão, visando simular ambientes de reservatório de hidrocarbonetos com anisotropia elétrica. Os objetivos deste trabalho são basicamente dois: fazer uma análise comparativa do grau de anisotropia de reservatórios laminados com relação a uma camada anisotrópica equivalente e, no desenrolar deste estudo, reavaliar alguns antigos e ainda não explicados efeitos presentes nos perfis de indução. Estes efeitos têm apenas uma sutil influência nos perfis, embora sejam importantes para uma clara compreensão dos fenômenos eletromagnéticos envolvidos na perfilagem. Pelos resultados pode-se verificar que ao reduzir progressivamente as espessuras das lâminas, os perfis do arranjo coaxial convergem para os da camada anisotrópica equivalente bem mais rápido do que os perfis do arranjo coplanar. Pode-se verificar também que, mesmo para lâminas extremamente finas, existe uma considerável diferença entre o índice de anisotropia, obtido com as ferrramentas triaxiais, com relação ao índice de anisotropia da camada equivalente.

Palavras-chave: perfilagem de poço, ferramentas multicomponentes, reservatórios laminados, anisotropia elétrica.

[1]Universidade Federal Rural da Amazônia, Instituto Ciberespacial, Av. Presidente Tancredo Neves, 2501, Terra Firme, 66077-530 Belém, PA, Brazil. Phone: +55(91) 3210-5109 – E-mails: paulo.carvalho@ufra.edu.br; prdcarvalhoufra@gmail.com

[2]Universidade Federal do Pará, Faculdade de Geofísica, Av. Presidente Tancredo Neves, 2501, Terra Firme, 66077-530, Belém, PA, Brazil. Phone: +55(91) 3201-7692; Phone-Fax: +55(91) 3201-7693; and National Institute of Science and Technology of Petroleum Geophysics, Universidade Federal da Bahia, Instituto de Geociências, sala 312-C, Campus de Ondina, 40170-115 Salvador, BA, Brazil – E-mails: cicero@ufpa.br; ciceroregis@gmail.com

INTRODUCTION

With the progressive exploitation of the main hydrocarbon reservoirs, it becomes a necessity to turn the attention to smaller and more complex reservoirs, which are usually made of relatively thin beds or laminae, but may have good permeability and porosity. Often, these deposits have good economic potential for having alternately source and reservoir rocks, besides having a large enough lateral extension to accumulate a considerable amount of oil and gas.

According to Gomes et al. (2002) "the deepwater reservoirs from Campos Basin comprise the most important petroleum accumulations in Brazil, holding approximately 80% of Brazil's oil reserves. These reservoirs can be very complex and heterogeneous, ranging from massive thick sands to highly laminated sand-shale sequences". Another possibility for laminated formations is the intercalation of porous laminae with other, less porous (cemented) ones, as is the case with some carbonaceous or aeolian deposits.

Before the year 2000, finely laminated reservoirs were underestimated or even ignored due to the geometric configuration of the coils in the traditional borehole electromagnetic induction logging tools. Since their invention (Doll, 1949), the coil arrangement was coaxial to the well axis and they overestimated the conductivity in environments where the conductive laminae of shale mask the presence of the resistive laminae of sandstone, saturated in oil.

From 2000 on, induction tools consist basically of a combination of a coaxial arrangement with two coplanar arrangements of coils, i.e. three sources and three sensors, with axes orthogonal to each other (Anderson et al., 2008). These tools are commercially referred to as triaxial (Krigshäuser et al., 2000) or multicomponent induction tools (Wang et al., 2003). The responses of the three arrangements of coils are simultaneously registered on multiple channels at multiple frequencies (tens of kHz) and source-sensor spacing. These probes were designed originally to investigate laminated reservoirs, and consequently, an anisotropic behavior.

Currently, besides being the main location tool of finely laminated reservoirs triaxial probes are also applied in many situations of asymmetric geometry, such as locating dissolution cavities (vugs) and fractured zones in the vicinity of the wells, monitoring invasion fronts in horizontal wells, and in any other asymmetrical geometry (Omeragic et al., 2015).

In this paper the logs were obtained by modeling laminated packages without considering the smoothing effects of the borehole and invasion zones. In this case, some subtle effects on the logs are intensified. These effects are of a geometric or/and electric nature, and some remained unexplained in the well logging literature.

The objective of this paper is twofold: to perform a quantitative analysis of the anisotropy level of a thinly laminated reservoir as compared to an equivalent anisotropic bed, and, in doing so, to revisit some of the old and unexplained effects that appear on the triaxial induction logs. These subtle effects may have only a faint influence on the logs themselves, but their study contribute to our understanding of the electromagnetic phenomena involved in the workings of the induction logging tools.

The objective of the comparative analysis is to find a lamina thickness from which the laminated formation models can be approximated by the response within a homogeneous intrinsically anisotropic bed within a relative difference of one percent (1%).

THEORY AND ANALYSIS METHOD

In the models with cylindrical symmetry studied here the six cross-coupled components of the triaxial tools are null. Thus, only the coaxial and coplanar vertical logs need to be modeled in one-dimensional (1D) laminated packages and in their equivalent anisotropic beds.

The transmitter coils can be represented as Vertical and Horizontal Magnetic Dipoles (VMD and HMD) in the coaxial and coplanar coil arrays, respectively, because the coil spacing (1.016 m or 40 in) is about 40 times larger than the radius of the coils (2.54 cm or 1 in).

Homogeneous isotropic media

According to Kaufman & Dashevsky (2003) in a homogeneous isotropic medium the transmitter coil produces only a single magnetic component normal to the receiver coil in the coaxial (H_z^{cx}) or coplanar (H_x^{cp}) arrays:

$$H_z^{cx} = \frac{M_T}{2\pi L^3}(1 - ikL)e^{ikL}, \tag{1}$$

$$H_x^{cp} = -\frac{M_T}{4\pi L^3}(1 - ikL - k^2L^2)e^{ikL}, \tag{2}$$

where a $e^{-i\omega t}$ time factor is used; $M_T = I_o n_T S_T$ is the transmitter dipole moment, I_o is the current amplitude, n_T is the number of turns in the transmitter coil, and S_T the cross-sectional area on the transmitter; L is the transmitter-receiver coil spacing; $i = \sqrt{-1}$; $k = \sqrt{i\omega\mu\sigma}$ is the wave number; f the linear frequency; $\omega = 2\pi f$ is the angular frequency; and μ is the magnetic permeability. According to the Faraday induction law, the electromotive force induced in each receiver coil is related to the

magnetic flux coupling generated by the magnetic field components described by Equations (1) and (2):

$$V^{cx} = i\omega\mu M_R H_z^{cx} = i\omega\mu M_R \frac{M_T}{2\pi L^3}(1-ikL)e^{ikL}, \quad (3)$$

$$V^{cp} = i\omega\mu M_R H_x^{cp} = -i\omega\mu M_R \frac{M_T}{4\pi L^3}(1-ikL-k^2L^2)e^{ikL} \quad (4)$$

where the $M_R = n_R S_R$ is called the receiver moment, n_R is the number of turns in the receiver coil, and S_R is the cross-sectional area of the receiver.

In order to make explicit the real (V_R^{cx} and V_R^{cp}) and the imaginary (V_X^{cx} and V_X^{cp}) parts of the Eqs. (3) and (4), let us rewrite the wave number as $k = (1+i)/\delta$, in which $\delta = \sqrt{2/\omega\mu\sigma}$ is the skin depth, and expand the complex exponential in terms of L/δ and, finally, define the proportionality constant $K = M_R M_T \omega^2 \mu^2 / \pi L$ which carries all the coil arrays parameters:

$$V_R^{cx} + iV_X^{cx} = K/4\big[\sigma + 2i/\omega\mu L^2 - 2/3(L/\delta)\sigma(1+i) + 1/2(L/\delta)^2\sigma i + 2/15(L/\delta)^3\sigma(1-i) + \ldots\big], \quad (5)$$

$$V_R^{cp} + iV_X^{cp} = -K/8\big[\sigma - 2i/\omega\mu L^2 - 4/3(L/\delta)\sigma(1+i) + 3/2(L/\delta)^2\sigma i + 8/15(L/\delta)^3\sigma(1-i) + \ldots\big]. \quad (6)$$

Ellis & Singer (2007) described in detail the terms in the brackets in the coaxial complex conductivity (Eq. 5). By following the same mathematical development, one gets the equivalent expression for the coplanar case (Eq. 6). Then, the terms in the same positions as in the previous Eq. (5) play the same roles: 1) the first term is real and it is simply the medium conductivity; 2) the second term is the direct transmitter-receiver mutual coupling which is independent of the medium conductivity and, being imaginary, it is 90° out of phase with the transmitter current and 3) the remaining terms of the series describe the skin effect on the complex signal, which represent the signal attenuation as well as its phase rotation (Ellis & Singer, 2007, p. 164).

Moran & Kunz (1962) define a "coaxial complex conductivity" by dividing Eq. (5) by the coaxial array constant $K/4$. Analogously, Carvalho & Verma (1999) presented a "coplanar complex conductivity" by dividing Eq. (6) by the coplanar array constant $K/8$:

$$\sigma_R^{cx} + i\sigma_X^{cx} = \sigma + 2i/\omega\mu L^2 - 2/3(L/\delta)\sigma(1+i) + 1/2(L/\delta)^2\sigma i + 2/15(L/\delta)^3\sigma(1-i) + \ldots, \quad (7)$$

$$\sigma_R^{cp} + i\sigma_X^{cp} = \sigma - 2i/\omega\mu L^2 - 4/3(L/\delta)\sigma(1+i) + 3/2(L/\delta)^2\sigma i + 8/15(L/\delta)^3\sigma(1-i) + \ldots. \quad (8)$$

The direct coupling is greater than the other terms by orders of magnitude, and it is always electronically removed from the measured signal. Therefore, the direct coupling term $2i/\omega\mu L^2$ must be removed from Eqs. (7) and (8), so that the complex conductivities signals come exclusively from the medium. The imaginary component is now called the reactive signal (σ_{XF}^{cx}). Eqs. (7) and (8) then become:

$$\sigma_R^{cx} + i\sigma_{XF}^{cx} = \sigma\big[1 - 2/3(L/\delta)(1+i) + 1/2(L/\delta)^2 i + 2/15(L/\delta)^3(1-i) + \ldots\big], \quad (9)$$

$$\sigma_R^{cp} + i\sigma_{XF}^{cp} = \sigma\big[1 - 4/3(L/\delta)(1+i) + 3/2(L/\delta)^2 i + 8/15(L/\delta)^3(1-i) + \ldots\big]. \quad (10)$$

In cases of relatively low conductivity ($\sigma < 0.1$ S/m) the first term in each of the series in Eqs. (9) (coaxial array) and (10) (coplanar array) is enough to estimate the conductivity of the medium, i.e., if $L/\delta \approx 0$ then $\sigma \approx \sigma_R^{cx} = \sigma_R^{cp}$. However, for conductivities ranging from 0.1 to 1 S/m it is necessary a first order skin effect correction in the resistive signals σ_R^{cx} and σ_R^{cp} by the factors $[1 - 2L/3\delta]$ and $[1 - 4L/3\delta]$, which are also present in the imaginary components. For conductivities above 1 S/m more terms of the series would be necessary, although there is no longer an exact correspondence between the real and imaginary components. According to Ellis & Singer (2007) in low conductivity environments this correspondence is good enough that, in actual logging, the tools measure the imaginary component to obtain and apply these "boosters" on the resistive signals of the Eqs. (9) and (10), generating the corrected signals

$$\sigma_c^{cx} = \sigma_R^{cx}/(1 - \sigma_{XF}^{cx}), \quad (11)$$

$$\sigma_c^{cp} = \sigma_R^{cp}/(1 - \sigma_{XF}^{cp}). \quad (12)$$

Figure 1 shows the apparent conductivities (resistive, reactive and boosted signals) versus the true conductivities of the homogeneous isotropic media for the coaxial and coplanar coil arrays.

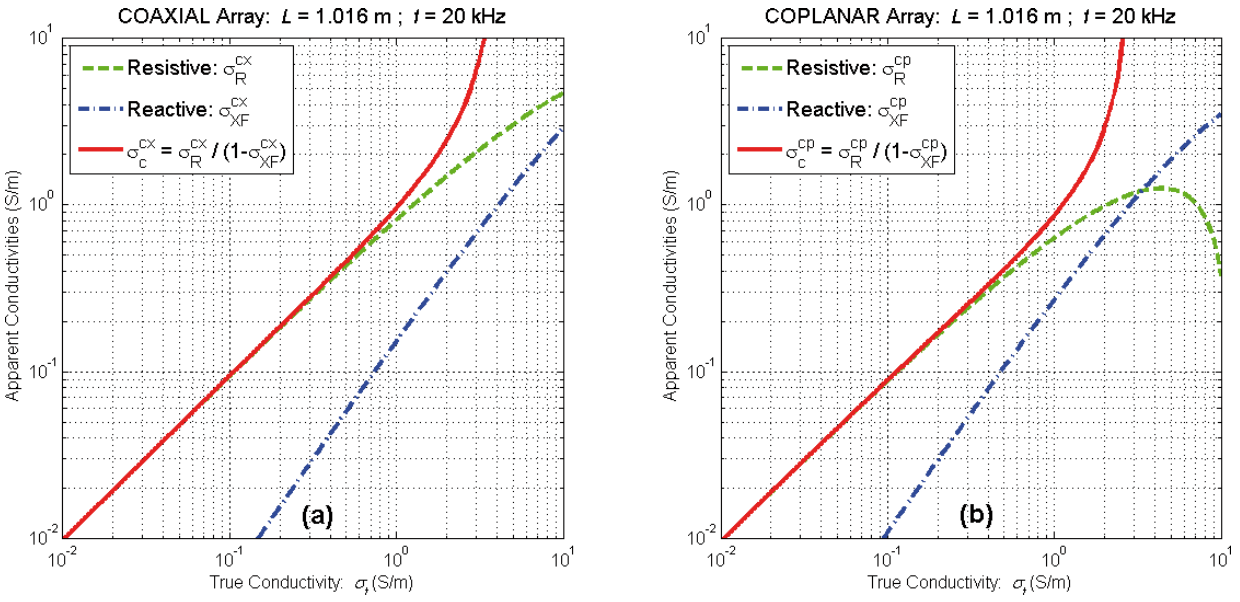

Figure 1 – Resistive (σ_R^{cx} and σ_R^{cp}), reactive (σ_{XF}^{cx} and σ_{XF}^{cp}) and corrected (σ_c^{cx} and σ_c^{cp}) signals of the coaxial (a) and coplanar (b) coil arrays in isotropic homogenous media.

The coplanar resistive signal σ_R^{cp} deviates from linearity much earlier (near $\sigma_t = 10^{-2}$ S/m) than of the coaxial resistive signal σ_R^{cx} (near $\sigma_t = 10^{-1}$ S/m). The skin effect correction in both signals almost recover the linearity in the boosted (or "corrected") signals (σ_c^{cx} and σ_c^{cp}) below 1 S/m which is the largest conductivity in the oil reservoir environments.

The complex conductivity (Eqs. 7 and 8) may also be written in terms of the magnetic fields (Eqs. 1 and 2) registered by coaxial and coplanar coil arrays:

$$\sigma_R^{cx} + i\sigma_X^{cx} = (2i/\omega\mu L^2)h_z^{cx}, \tag{13}$$

$$\sigma_R^{cp} + i\sigma_X^{cp} = (-2i/\omega\mu L^2)h_x^{cp}, \tag{14}$$

where $h_z^{cx} = (1 - ikL)e^{ikL}$ and $h_x^{cp} = (1 - ikL - k^2L^2)e^{ikL}$ are the secondary magnetic fields which come exclusively from the medium, i.e., without the transmitter/receiver mutual coupling terms.

Homogeneous anisotropic media

Although all the analysis presented above is for homogeneous isotropic media, in actual induction logging it is common practice to apply Eqs. (13) and (14) to fields from more complex media such as anisotropic or inhomogeneous media.

In the comparative analysis performed in this paper, the logs were simulated in thinly laminated packages and in intrinsically anisotropic beds. The main difference between these two models is in the form of representing the electrical conductivity: in the thinly laminated formations there are two distinct and alternate scalar conductivities, σ_1 and σ_2, whereas in the anisotropic bed the conductivity is a 3×3 tensor $\tilde{\sigma}$:

$$\tilde{\sigma} = \begin{bmatrix} \sigma_{xx} & \sigma_{yx} & \sigma_{zx} \\ \sigma_{xy} & \sigma_{yy} & \sigma_{zy} \\ \sigma_{xz} & \sigma_{yz} & \sigma_{zz} \end{bmatrix}. \tag{15}$$

However, when the anisotropic medium has Transversely Isotropic layers with a Vertical axis of symmetry (TIV), in which the main anisotropy directions are the same as the coordinate axes, the off-diagonal terms are all zeros, $\sigma_{xx} = \sigma_{yy} = \sigma_h$, and $\sigma_{zz} = \sigma_v$. Thus, the conductivity tensor (Eq. 15) reduces to:

$$\tilde{\sigma} = \begin{bmatrix} \sigma_h & 0 & 0 \\ 0 & \sigma_h & 0 \\ 0 & 0 & \sigma_v \end{bmatrix}. \tag{16}$$

This type of anisotropic medium (TIV) has a characteristic parameter named coefficient of anisotropy, defined as the ratio between the horizontal (σ_h) and the vertical (σ_v) conductivities, which is a useful measure of the degree of anisotropy:

$$\lambda^2 = \sigma_h/\sigma_v. \tag{17}$$

Laminated formation and anisotropic bed

In 1D layered media, in which the presence of the borehole and the invasion zones are neglected, the formulae for the magnetic field components are expressed in terms of improper integrals

due to the inverse Hankel transform, which are solved numerically. This is true for the fields generated by vertical (VMD) and horizontal (HMD) Magnetic Dipoles within a laminated formation (Anderson et al., 1986; Carvalho et al., 2010) as well as for the magnetic field components generated by an HMD in an anisotropic bed bordered by two half-spaces (Kaufman & Dashevsky, 2003).

Kaufman & Dashevsky (2003) deduced through current density distribution and Anderson et al. (2008) show through circuit theory (parallel and series resistors) an identical relation between the horizontal and vertical conductivities of the homogeneous anisotropic media and the conductivities of the thinly laminated medium formed by two alternating and distinct laminae (σ_1 and σ_2) when their thicknesses are less than the tool's vertical resolution:

$$\sigma_h = \sigma_1 V_1 + \sigma_2 V_2, \tag{18}$$

$$\sigma_v = (V_1/\sigma_1 + V_2/\sigma_2)^{-1}, \tag{19}$$

where V_1 and V_2 are the volume fractions of each material which are obtained by spectroscopy probe. Thus, the sand laminae resistivity can be calculated from horizontal and vertical resistivities (Eqs. 18 and 19) and Archie's equation can be used to estimate the water saturation in the thinly laminated reservoir (Clavaud et al., 2005).

To perform a quantitative analysis of the anisotropy level of a thinly laminated reservoir as compared to an equivalent anisotropic bed, the following examples illustrate the simplest case of equal volume fractions ($V_1 = V_2 = 0.5$). In this study the laminae thicknesses are progressively reduced until the laminated formation has the same behavior of an anisotropic bed. Thus, in this limit Eqs. (18) and (19) simplify to:

$$\sigma_h = (\sigma_1 + \sigma_2)/2, \tag{20}$$

$$\sigma_v = 2(\sigma_1\sigma_2)/(\sigma_1 + \sigma_2). \tag{21}$$

The anisotropy coefficient of the equivalent bed can be written as a function of the thin laminae conductivities by applying Eqs. (20) and (21) in Eq. (17)

$$\lambda^2 = \sigma_h/\sigma_v = (\sigma_1 + \sigma_2)^2/(4\sigma_1\sigma_2). \tag{22}$$

Kaufman & Dashevsky (2003) show that at low frequency range, that is $\omega \rightarrow 0$ or $L/\delta \ll 1$, the quadrature part (imaginary component) of the secondary magnetic fields (without the mutual coupling term) registered by coaxial ($Q\{h_{zz}^{cx}\}$) and coplanar ($Q\{h_{xx}^{cp}\}$) coil arrays are directly proportional to the horizontal (σ_h) and vertical (σ_v) conductivities, respectively. Thus, the ratio between them yields a structural anisotropy index (λ_R^2), which is also obtained by the ratio between the coaxial (σ_R^{cx}) and the coplanar (σ_R^{cp}) resistive signals, since they are obtained by multiplying the respective field components by the same proportionality constant (Eqs. 13 and 14):

$$\lambda_R^2 = Q\{h_{zz}^{cx}\}/Q\{h_{xx}^{cp}\} = \sigma_R^{cx}/\sigma_R^{cp} \cong \sigma_h/\sigma_v. \tag{23}$$

However, in order to compare the laminated formation responses with the equivalent anisotropic bed, yet another structural anisotropy index (λ_c^2) was used, obtained through the ratio of the boosted signals of the coaxial (σ_c^{cx}) and coplanar (σ_c^{cp}) coil arrays. This index is closer to the anisotropy coefficient of the equivalent bed:

$$\lambda_c^2 = \sigma_c^{cx}/\sigma_c^{cp}\,. \tag{24}$$

In modern induction logging this anisotropy index is a useful measurement for determining the level of resistivity anisotropy of the laminated formations. As a general rule, when this ratio is higher than five it alerts the log analyst to look for a potential pay laminated reservoir (Anderson et al., 2008). A classic example occurred in the Krishna-Godavari basin (west coast of India) where the thin sand-shale turbidite reservoirs were overlooked or underestimated by more than 60% by traditional induction tools, which used only the coaxial coil array (Anderson et al., 2008).

RESULTS AND DISCUSSIONS

From here on the results are presented in the form of the standard wireline services resistivity logs. The next examples use shale resistivity as $\rho_{sh} = 1$ ohm-m and sandstone resistivity as $\rho_{sd} = 5$ ohm-m, following the same values used in Anderson (1986). When the laminae are infinitely thin these values are applied in Eqs. (20) and (21) to obtain the horizontal and vertical resistivities $\rho_h = 1.67$ ohm-m and $\rho_v = 3$ ohm-m, for an equivalent anisotropic bed with an anisotropy coefficient $\lambda^2 = \rho_v/\rho_h = 1.8$, which is close to the typical contrast for actual logging situations ($\lambda^2 \cong 2$), according to Anderson et al. (1990).

Figure 2 shows the three coaxial and coplanar signals (resistive, reactive and corrected) in a thick (10.5L) laminated package with 21 laminae, each with thickness L/2. The coplanar signals show a more prominent oscillation and suffer the strongest adjacent bed and skin effects. They also show a greater sensitivity to the resistive laminae (hydrocarbons-bearing sands), whereas the coaxial signals suffer a stronger effect of the conductive laminae (shales), which mask the presence of the resistive laminae.

Polarizations "horns" appear in the coplanar profiles against the layer boundaries, especially on the resistive signal. These

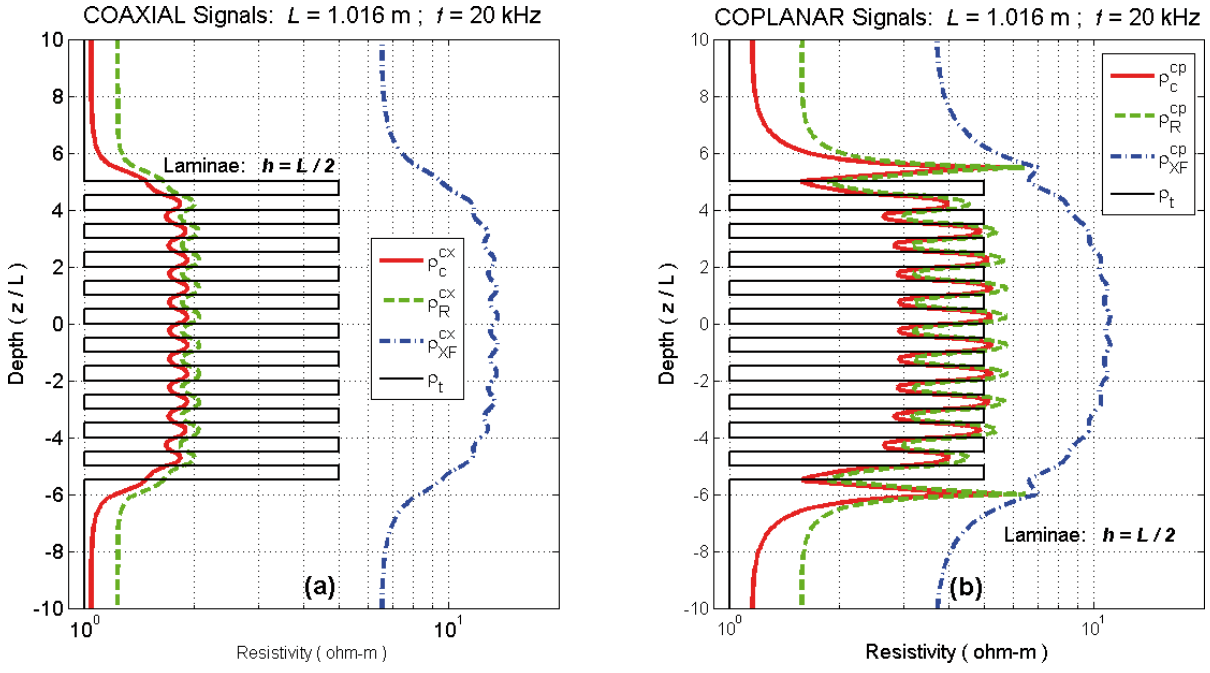

Figure 2 – Resistive (ρ_R^{cx} and ρ_R^{cp}), reactive (ρ_{XF}^{cx} and ρ_{XF}^{cp}) and corrected (ρ_c^{cx} and ρ_c^{cp}) signals of the coaxial (a) and coplanar (b) arrays in a laminated ($h = L/2$) model.

horns are caused by the building up of charges at the boundaries, which is related to the discontinuity of the normal component of the electric field at the interfaces.

Howard & Chew (1992) showed theoretically and Carvalho & Verma (1998) showed experimentally, through test tank measurements, that these oscillations on the logs are damped if the presence of the borehole and invasion are taken into account. The build-up of surface charges acts like a secondary transmitter generating a signal in the vicinity of the interfaces. According to Anderson et al. (1990), "since the horn is located directly at the bed boundary, it is a high bed boundary indicator for large resistivity contrasts in steeply dipped beds". However, despite this possible advantage, the frequent presence of these horns in the coplanar logs was a strong reason for them to be considered undesirable until as recently as the year 2000.

In the following results only the corrected (boosted) signals are shown, which present all the geometric and electromagnetic effects that will be discussed, and which are, after all, the final product delivered by the resistivity tools in actual logging.

Figure 3 shows the coaxial and coplanar corrected logs within two thick (10L) models: 1) a laminated formation (red lines) and 2) an equivalent anisotropic bed (blue lines). These logs are right in the middle of the models ($z = 0$) with the depth raging from –2L to 2L, i.e., well away from the boundaries to the adjacent infinite half-spaces above and below.

In vertical coaxial logs the induced currents flow only parallel to the lamina planes, so that these logs are strongly affected by the conductive laminae (1 ohm-m), and the packages behaves as an isotropic bed with resistivity equal to the bed's horizontal resistivity $\rho_h = 1.67$ ohm-m. With the progressive reduction of the laminae thicknesses, $h = L/n$ with n ranging from 2 to 10 in Figure 3, the coaxial logs for both models are almost indistinguishable for thicknesses less than L/3.

With the reduction of the laminae thicknesses, the coplanar logs show two alternating features within the laminated formation: "smooth" for even values of n (L/2, L/4, L/6, L/8 and L/10) and "angular" for odd values of n (L/3, L/5, L/7 and L/9).

Anderson et al. (1990) also show these two response patterns (smooth and angular) in the coaxial logs within laminated formation crossed by different dip angles, although they do not explain the reason for these apparent strange responses. However, in vertical logs, as in the examples in this paper, the coaxial responses are always smooth because there is no discontinuous electric field, and no polarization effects.

In the coplanar smooth logs (even n) the transmitter coil is always in a layer with the same conductivity as the receiver coil and the number of interfaces between them is even. Consequently, the interface polarizations between them tend to cancel out, and the polarization effects to disappear. However, in the coplanar angular logs (odd n), transmitter and receiver coils are always at

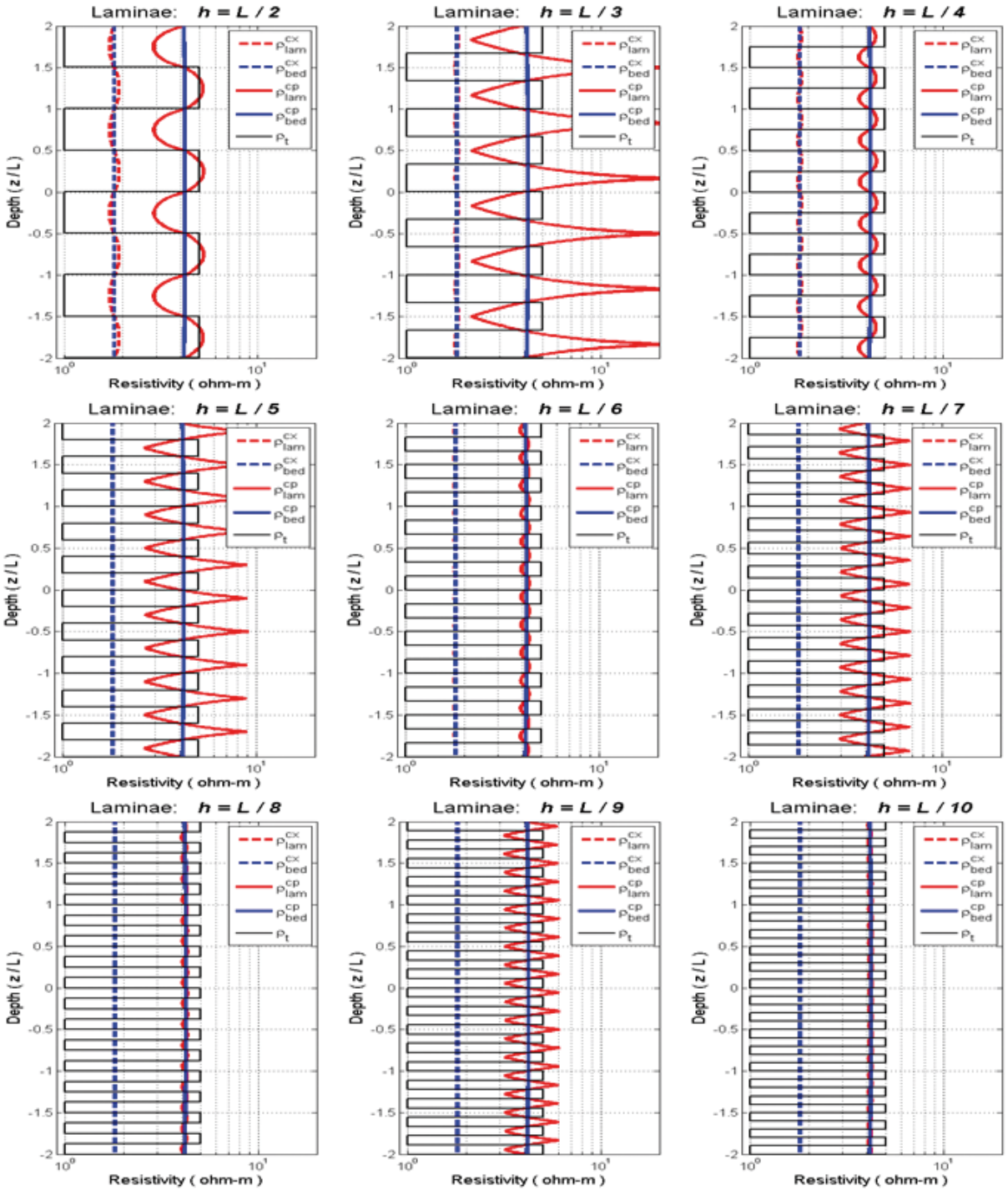

Figure 3 – Evolution of the coaxial and coplanar corrected logs (ρ_c^{cx} and ρ_c^{cp}) within a laminated formation (oscillating red lines) in relation to its equivalent anisotropic bed (straight blue lines).

different conductivities and the number of interfaces between them is odd. Therefore, the net polarization between them is not null and the horning effects appear in this case as a cusped feature. These polarization effects affect not only the shape (smooth to angular) but also the magnitude of the oscillations of the coplanar logs, so that, for example, going from laminae thicknesses L/6 to L/7 the magnitude increases, even though the laminae in the latter case are thinnest.

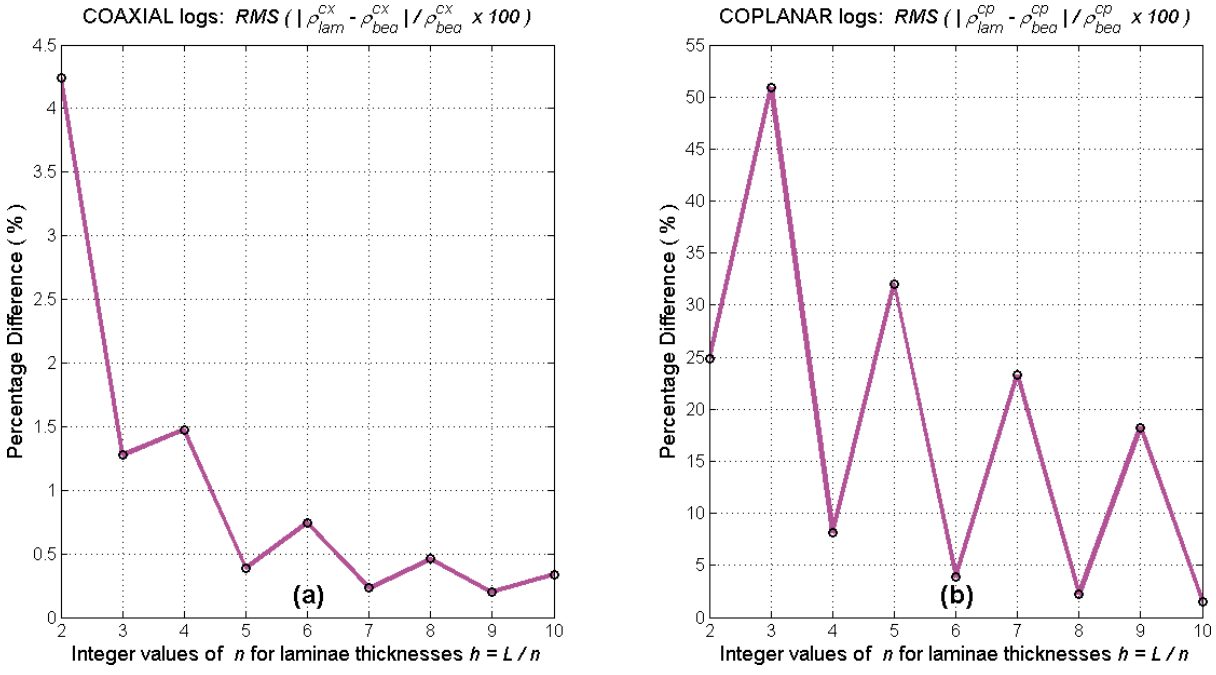

Figure 4 – Relative difference (%) between the laminated formation and the equivalent anisotropic bed responses to the coaxial (a) and coplanar (b) corrected logs with reduction of the laminae thicknesses.

In some laminae thicknesses such as L/3, L/5, L/6 and L/9, there is a curve reversal with respect to the model for both coaxial and coplanar logs while in others there is a perfect correlation with the model. Anderson (1986) shows similar results in coaxial logs and comments that "reflections from bed boundaries located within the coil spacing make impossible for the electromagnetic waves to contain correct information about the media", which is a true enough statement that does not really explain the phenomenon, which seems to stem from purely geometrical effects of the relative positions of the transmitter and the receiver within the laminae, and which is present in both coil arrays.

To summarize the results for the whole sequence of models, Figure 4 shows the Root Mean Square (RMS) of the relative difference (%) between the laminated formation (red solid lines) and the anisotropic bed (dashed blue lines) responses of the coaxial and coplanar logs showed in Figure 3.

The coaxial logs from the laminated formation converge to the homogeneous anisotropic bed much earlier than the coplanar logs. If relative difference of 1% is taken as an indicator of convergence between both models, Figure 4 shows that this convergence occurs around L/5 in the coaxial logs, whereas in the coplanar logs it comes later, so that in L/9 and L/10 this difference is still 18.22% (odd n) and 1.454% (even n), respectively.

A surprising effect in the coaxial logs and exactly opposite to what happens in the coplanar logs can be clearly seen in Figure 4-a: the magnitude of the oscillation in each of the odd n cases is smaller than that in the following even n case (L/3 and L/4, for example), despite the fact that in the latter case the laminae are less thick. There aren't any polarization charges in these vertical coaxial logs. The only difference between the two cases is that in the even n cases the material volumes (shale and sand) between the transmitter and the receiver coils are always constant and identical ($V_{sh} = V_{sd} = 0.5$), regardless of the laminae thicknesses, whereas in the odd cases they change according to the position of the coils inside the package, oscillating around an average value of 0.5, so that the fields propagate in a medium that is, on average, more or less conductive depending on the sonde position. As the laminae get thinner and thinner, all oscillations tend to disappear and the curves tend to the value of the equivalent horizontal resistivity.

Figure 5 shows again the RMS of the relative difference (%) between the laminated formation and the anisotropic bed only for the coplanar logs. The laminae thicknesses is now reducing from L/2 to L/1001 to represent oil reservoirs in sand-shale-silt sequences in which the laminae thicknesses are in the millimeter range, well below the minimum vertical resolution available from resistivity tools (Anderson et al., 2008). The percentage differences of the even n (dashed line) and odd n (solid line) cases decay exponentially with the reduction of the laminae thicknesses and they reach the reference value of 1% around L/12 (1.014%)

and L/165 (1.007%), respectively. The even case curve reaches 0.1134% at L/40 whereas the odd case curve reaches 0.1659% only at L/1001.

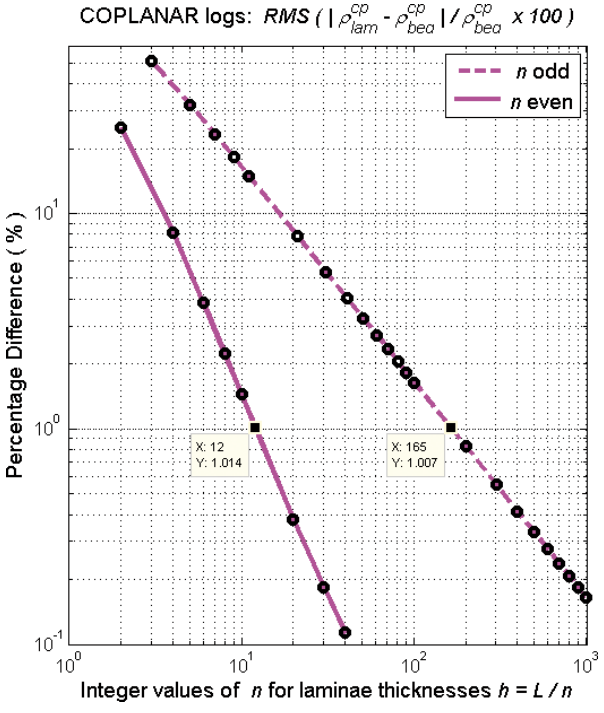

Figure 5 – Relative difference (%) between the laminated formation and the equivalent anisotropic bed responses to the coplanar corrected logs with reduction of the laminae thicknesses.

Figure 6 shows the coaxial (ρ_c^{cx}) and coplanar (ρ_c^{cp}) corrected resistivity logs and the structural anisotropy logs ($\lambda_c^2 = \rho_c^{cp}/\rho_c^{cx}$) within three distinct thinly laminated formations with laminae thicknesses L/11 (a), L/101 (b) and L/1001 (c). All three coaxial logs (blue dash-dot lines) are practically straight and indistinguishable from each other, whereas the coplanar logs (red solid lines) and, therefore, the anisotropy logs oscillate with progressively less amplitude, to the point where the oscillations virtually disappear for laminae thicknesses less than a hundredth of the coil spacing L. The Root Mean Square (RMS) of the resistivity anisotropy logs is around $RMS(\lambda_c^2) \cong 2.33$, which is approximately 28% higher than the anisotropy coefficient $\lambda^2 = \sigma_h/\sigma_v = 1.8$ of the equivalent bed.

This considerable difference between the structural anisotropy index and the anisotropy coefficient, even for such thin lamina thickness, steams chiefly from the use of a frequency (20 kHz) which is far from the ideal approach condition required by the formula (Eq. 23) of a frequency close to zero (Kaufman & Dashevsky, 2003).

Figure 7 shows how the structural anisotropy of the thinly laminated reservoirs changes with the sand-shale resistivities. In laminated reservoir environments the sand resistivity may vary from 2.5 to 25 ohm-m, due mainly to the sandstone compaction and oil saturation (Anderson et al., 1986; 1990). The points A and B show that a relatively small variation in the shale resistivity causes a large change in the anisotropy index, i.e., when the shale resistivity varies from 1 (solid line) to 2 ohm-m (dashed line) for a 20 ohm-m sand resistivity the anisotropy index reduces from 12 to 4, approximately.

According to Anderson et al. (2008), in actual induction logging this structural anisotropic index yields useful information, so much so that when it is higher than five (horizontal black dash-dot line), it alerts the log analyst to look for a potential pay laminated reservoir. However, one must be careful in this interpretation, because it is possible that a laminated pay reservoir generates a value of the structural anisotropy index below the reference line ($\lambda_c^2 < 5$) if the main reason for the resistivity anisotropy is the oil concentration in the sandstone laminae, as illustrated by point B in Figure 7.

CONCLUSIONS

This paper presents an analysis of vertical logs for the coaxial and coplanar coil arrays, present in the modern triaxial induction tools, within one-dimensional (1D) laminated reservoir models and their equivalent anisotropic bed, in which the presence of the borehole and the invasion zones are neglected.

The results reproduce some well known characteristics of the coplanar logs: for example, polarization "horns" are obtained in front of the laminated package boundaries. These horns could be considered good indicators of the interface positions. However, the frequent presence of these "horns" in the coplanar logs was a strong reason for them to be considered undesirable until as recently as the year 2000. Another point observed in the results is that the skin effect is strongest in the coplanar responses, but this handicap is partially compensated by using the reactive component to obtain and apply a "booster" on the resistive component.

Based on the comparative study between the responses from a laminated reservoir and its equivalent anisotropic bed, for a coil spacing L, we conclude that:

1. Coplanar logs are more sensitive to detect and delineate thinly laminated reservoirs because of the electric charge accumulation on the laminae interfaces. As the laminae thicknesses (L/n) are reduced the coplanar logs show two alternating features within the laminated formation: "smooth" for even values of n and "angular" for odd values of n. In the even n case the number of interfaces between transmitter-receiver coils is even, consequently, the

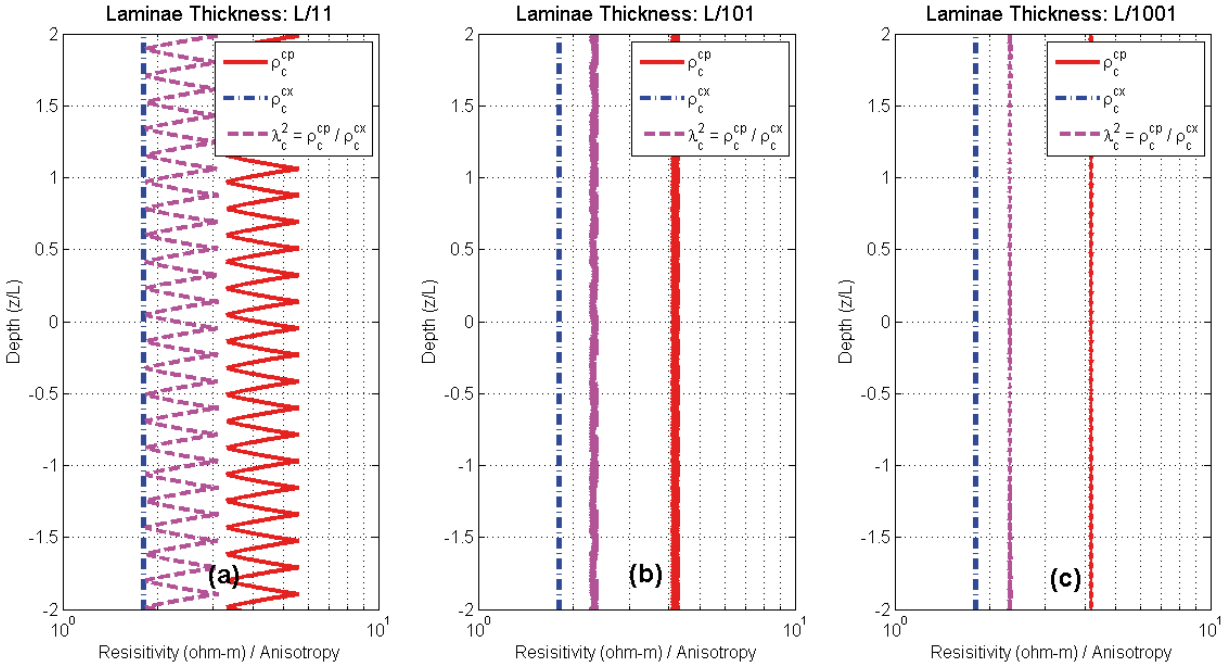

Figure 6 – Coaxial and coplanar resistivity logs and the resistivity anisotropy logs within three laminated formations with laminae thicknesses: L/11 (a); L/101 (b); and L/1001 (c).

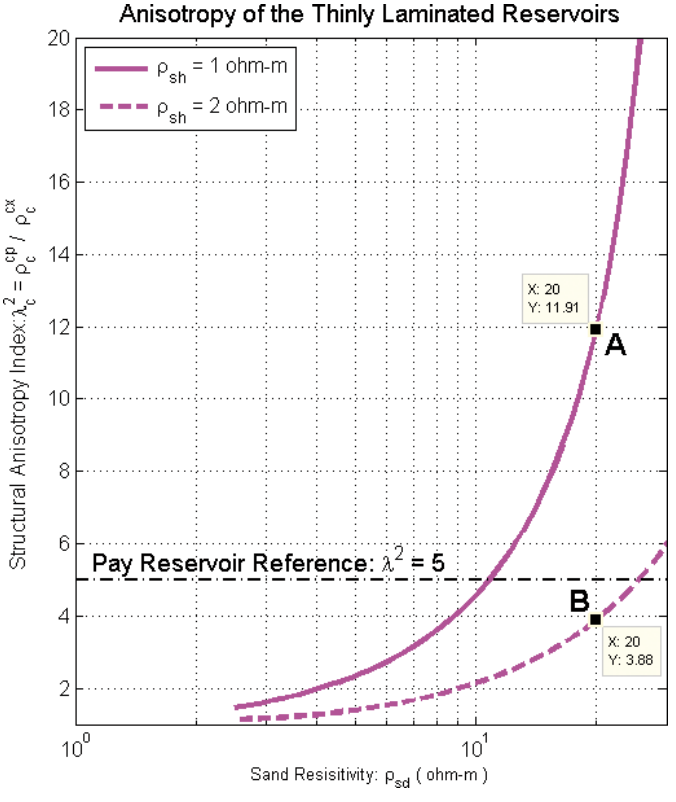

Figure 7 – Structural anisotropy index within thinly laminated formations ($h = L/165$) versus the sand-shale laminae resistivities.

polarization effects tend to cancel out and disappear. However, in the odd n cases the number of interfaces between the transmitter-receiver coils is odd, consequently the net polarization between them is not null and the polarization effects appear as a cusped feature. Because of these polarizations, the oscillation magnitude in any odd n case is always greater than in the preceding even case $(n-1)$, despite the fact that the laminae in the former are thinnest;

2. The coaxial logs in the laminated formation converge to the equivalent anisotropic bed response much sooner than the coplanar logs, i.e., the convergence to within 1% occurs around L/5 in the coaxial logs whereas in the even n and odd n cases in the coplanar logs they occur around L/12 and L/165, respectively;

3. A surprising effect occurs in the coaxial logs where the magnitude of the log oscillation in each of the odd n cases is smaller than that in the following even n case, despite the fact that in the latter the laminae are less thick. There aren't any polarization charges in these vertical coaxial logs and the only difference between the two cases is that for even n the sand-shale volumes between the transmitter and the receiver coils are always constant and identical $(V_{sh} = V_{sd} = 0.5)$ whereas in the odd cases these volumes change according to the position of the coils inside the package, with an average of 0.5;

4. In some laminae thicknesses there is a curve reversal with respect to the model for both coaxial and coplanar logs while in others there is a perfect correlation. These curve reversals seem to stem from purely geometrical effects of the relative positions of the transmitter and the receiver within the laminae, which are present in both coil arrays;

5. There is a considerable difference between the structural anisotropy index and the anisotropy coefficient, even for extremely thin laminae thicknesses. This difference is chiefly due to the relatively high frequency used in induction logging (tens of kHz) which is far from the ideal approach condition that is a frequency close to zero;

6. It is possible that a laminated pay reservoir generates a value of the structural anisotropy index below the reference value (five) if the main reason for the resistivity anisotropy is the oil concentration in the sandstone laminae.

ACKNOWLEDGEMENTS

Paulo Carvalho thanks the CAPES (Coordenação de Aperfeiçoamento de Pessoal de Nível Superior) for the post-doctoral fellowship in the "Programa de Pós-Graduação em Geofísica" of the Universidade Federal do Pará (CPGf/UFPA). Régis is recipient of the CNPq Research Grant.

REFERENCES

ANDERSON BI. 1986. The analysis of some unsolved induction interpretation problems using computer modeling. In: Transactions of the SPWLA, paper II, 27th Annual Logging Symposium, Houston, USA.

ANDERSON BI, SAFINYA, KA & HABASHY T. 1986. Effects of dipping beds on the response of induction tools. In: Annual Technical Conference and Exhibition. New Orleans, USA. Annals SPE.

ANDERSON BI, BORNER S, LÜLING MG & ROSTHAL R. 1990. Response of 2-MHz LWD resistivity and wireline induction tools in dipping beds and laminated formations. In: Transactions of the SPWLA, paper A, 31st Annual Logging Symposium, Lafayette, Louisiana, USA.

ANDERSON BI, BARBER T, BASTIA R, CLAVAUD JB, COFFIN B, DAS M, HAYDEN R, KLIMENTOS T, MINH CC & WILLIAMS S. 2008. Triaxial induction – A new angle for an old measurement. Oilfield Review, 20(2): 64–84.

CARVALHO de PR & VERMA OP. 1998. Induction tool with a coplanar coil system. The Log Analyst, 39(6): 48–53. https://www.onepetro.org/journal-paper/SPWLA-1998-v39n6a3

CARVALHO de PR & VERMA OP. 1999. Coplanar coils response in a borehole. In: 6th International Congress of the Brazilian Geophysical Society. Rio de Janeiro, RJ, Brazil. http://earthdoc.eage.org/publication/publicationdetails/?publication=47940

CARVALHO de PR, SANTOS dos WG & RÉGIS CTR. 2010. Fundamentals of coaxial and coplanar coil arrays in induction tools. Brazilian Journal of Geophysics, 28(1): 19–36. http://dx.doi.org/10.1590/S0102-261X2010000100002

CLAVAUD JB, NELSON R, GURU UK & WANG H. 2005. Field example of enhanced hydrocarbon estimation in thinly laminated formation with a triaxial array induction tool: a laminated sand-shale analysis with anisotropic shale. In: Transactions of the SPWLA, paper WW, 46th Annual Logging Symposium, New Orleans, USA.

DOLL HG. 1949. Introduction to induction logging and application to logging of wells drilled with oil-based mud. Journal of Petroleum Technology, 1(6): 148–162.

ELLIS DV & SINGER JM. 2007. Well Logging for Earth Scientists. 2nd ed., Springer. 692 pp.

GOMES RM, DENICOL PS, CUNHA AMV da, SOUZA MS de, KRIGSHÄUSER BE, PAYNE JC & SANTOS A. 2002. Using multicomponent induction log data to enhance formation evaluation in deepwater reservoirs from Campos Basin, offshore Brazil. In: Transactions of the SPWLA, paper N, 43rd Annual Logging Symposium, 2-5 June, Oiso, Japan.

HOWARD AQ Jr. & CHEW WC. 1992. Electromagnetic borehole fields in a layered dipping-bed environment with invasion. Geophysics, 57(3): 451–465.

KAUFMAN AA & DASHEVSKY YA. 2003. Principles of induction logging. Amsterdam Elsevier Publishers. 643 pp.

KRIGSHÄUSER BE, FANINI O, FORGANG S, ITSKOVICH G, RABINOVICH M, TABAROVSKY L & YU L. 2000. A new multicomponent induction logging tool to resolve anisotropic formations. In: Transactions of the SPWLA, paper D, 41st Annual Logging Symposium, 4-7 June, Dallas, Texas, USA.

MORAN JH & KUNZ KS. 1962. Basic theory of induction logging and application to study of two-coil sondes. Geophysics, 27(6): 829–858.

OMERAGIC D, BAYRAKTAR Z, THIEL M, HABASHY T, ALATRACH S & SHRAY F. 2015. Triaxial Induction Interpretation in Horizontal Wells: Mapping Boundaries, Characterizing Anisotropy and Fractures. In: Transactions of the SPWLA, paper I, 56th Annual Logging Symposium, 18-22 July, Long Beach, California, USA.

WANG T, YU L & FANINI O. 2003. Multicomponent induction response in a borehole environment. Geophysics, 68(5): 1510–1518.

Recebido em 17 janeiro, 2017 / Aceito em 4 maio, 2017
Received on January 17, 2017 / Accepted on May 4, 2017